

# Exploration of a large-scale reconstructed structure on GaN(0001) surface by Bayesian optimization

Kusaba, Akira

Research Institute for Applied Mechanics, Kyushu University

Kangawa, Yoshihiro

Research Institute for Applied Mechanics, Kyushu University

Kuboyama, Tetsuji

Computer Centre, Gakushuin University

Oshiyama, Atsushi

Institute of Materials and Systems for Sustainability, Nagoya University

<https://hdl.handle.net/2324/7173557>

---





出版情報 : Applied Physics Letters. 120 (1), pp.021602-, 2022-01-10. AIP Publishing  
バージョン :

権利関係 : © 2022 Author(s). Published under an exclusive license by AIP Publishing.



RESEARCH ARTICLE | JANUARY 10 2022

## Exploration of a large-scale reconstructed structure on GaN(0001) surface by Bayesian optimization

A. Kusaba  ; Y. Kangawa  ; T. Kuboyama  ; A. Oshiyama 



*Appl. Phys. Lett.* 120, 021602 (2022)

<https://doi.org/10.1063/5.0078660>



### An innovative I-V characterization system for next-gen semiconductor R&D

Unique combination of ultra-low noise sourcing + high-sensitivity lock-in measuring capabilities

[Learn more](#)



# Exploration of a large-scale reconstructed structure on GaN(0001) surface by Bayesian optimization

Cite as: Appl. Phys. Lett. **120**, 021602 (2022); doi: [10.1063/5.0078660](https://doi.org/10.1063/5.0078660)

Submitted: 14 November 2021 · Accepted: 26 December 2021 ·

Published Online: 10 January 2022



View Online



Export Citation



CrossMark

A. Kusaba,<sup>1</sup> Y. Kangawa,<sup>1</sup> T. Kuboyama,<sup>2</sup> and A. Oshiyama<sup>3</sup>

## AFFILIATIONS

<sup>1</sup>Research Institute for Applied Mechanics, Kyushu University, Kasuga, Fukuoka 816-8580, Japan

<sup>2</sup>Computer Centre, Gakushuin University, Toshima-ku, Tokyo 171-8588, Japan

<sup>3</sup>Institute of Materials and Systems for Sustainability, Nagoya University, Chikusa-ku, Nagoya 464-8601, Japan

<sup>a)</sup> Author to whom correspondence should be addressed: [kusaba@riam.kyushu-u.ac.jp](mailto:kusaba@riam.kyushu-u.ac.jp)

## ABSTRACT

GaN(0001) surfaces with Ga- and H-adsorbates are fundamental stages for epitaxial growth of semiconductor thin films. We explore stable surface structures with a nanometer scale by the density-functional calculations combined with Bayesian optimization and reach a single structure with satisfactorily low mixing enthalpy among hundreds of thousand possible candidate structures. We find that the obtained structure is free from any postulated high symmetry previously introduced by human intuition, satisfies an electron counting rule locally, and shows a complex adsorbate arrangement, reflecting characteristics of nitride semiconductors. The proposed scheme toward a high-resolution surface phase diagram contributes to a more precise design of GaN epitaxial growth conditions, especially the ratio of Ga and H partial pressures.

Published under an exclusive license by AIP Publishing. <https://doi.org/10.1063/5.0078660>

Nitride semiconductors, which are already premier materials in optoelectronics,<sup>1,2</sup> are now emerging in power electronics due to their superior physical properties to Si.<sup>3</sup> GaN vertical metal–oxide–semiconductor devices show efficient energy conversion,<sup>4</sup> and AlGaIn/GaN high-electron mobility transistors are also gradually spreading in the market,<sup>5</sup> inferring that nitrides contribute to sustain our energy-saving society. However, to guarantee the expected high performance of such power devices, it is necessary to forge high-quality epitaxial films of GaN. Despite many experimental efforts in this decade,<sup>6,7</sup> the current quality of GaN crystalline films is unsatisfactory for replacing Si power devices in the market.

Improvement in the epitaxial growth technique has been pursued based on empirical knowledge and experimental trials and errors that require a huge amount of time and resources. It may be more promising to obtain knowledge of atomistic processes in growth phenomena first and then design optimum conditions for epitaxial growth. To unveil the growth phenomena, atom-scale identification of the surfaces on which atomic reactions take place is an essential prerequisite. However, such identification is difficult in experiments since harsh environments, such as high temperatures during metal-organic vapor phase epitaxy (MOVPE), render sophisticated experimental techniques inapplicable. A computational approach based on the first

principles of quantum theory is an alternative and reliable way to identify growth surfaces.

First-principle calculations within density-functional theory (DFT) have indeed been performed for the reconstruction of GaN surfaces.<sup>8–12</sup> Furthermore, recognizing that the growth surface is in equilibrium with the gas phase with a particular temperature and partial pressure of each molecular species under growth conditions, an approach combining DFT surface energies with thermodynamics of the gas phase has been proposed.<sup>13</sup> By this approach, the phase diagram of the surface structures in the space of the growth temperature and source-gas pressure is obtained, and our knowledge of the growth surface is expanded.<sup>14–16</sup> Unfortunately, the conclusions obtained in the past are based on rather small-scale DFT calculations by imposing short-range periodicity, e.g., by using a  $(2 \times 2)$  lateral cell. What is really necessary is the identification of the atomic structures of a wide range, at least nanometer scale, of growth surfaces, which presumably lack periodicities within the range.

More specifically, by using the above approach where DFT calculations for  $(2 \times 2)$  lateral cells are combined with thermodynamics, Kusaba *et al.*<sup>17</sup> identified the GaN(0001) growth surface in MOVPE. The most thermodynamically favorable surface is either the Ga adatom surface ( $\text{Ga}_{\text{ad}}$  hereafter) in which a single Ga adatom is

adsorbed on the so-called T4 site (see Fig. 1) or the hydrogen-covered surface (3Ga–H hereafter) in which three Ga–H bonds are formed (Fig. 1), depending on the balance of Ga and H<sub>2</sub> partial pressures during growth. Both structures satisfy electron counting rule (ECR):<sup>18</sup> All electrons in cation dangling bonds that are energetically unfavorable are transferred to the newly emerged Ga–Ga or Ga–H bonds. The satisfactions of ECR on Ga<sub>ad</sub> and 3Ga–H correspond to their particular

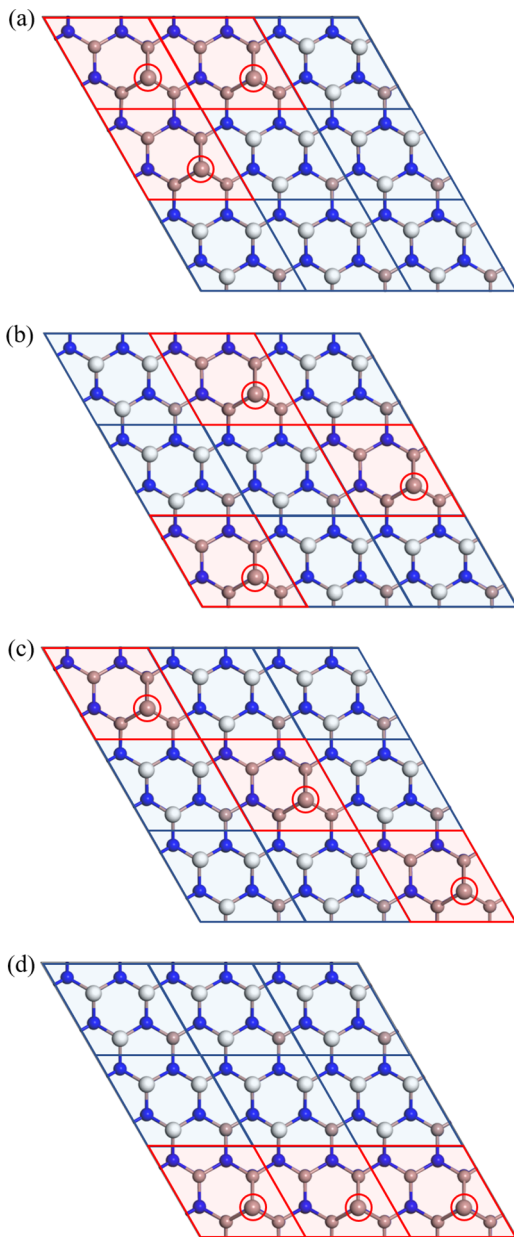


**FIG. 1.** (a)–(d) Top views of the baseline (6 × 6) surface models constructed by the different arrangements of the 3Ga–H (2 × 2) structure (blue tiles) and Ga<sub>ad</sub> (2 × 2) structure (red tiles). Brown, blue, and white atoms correspond to Ga, N, and H, respectively.

coverages of Ga and H, i.e.,  $\theta_{\text{Ga}} = 0.25$  and  $\theta_{\text{H}} = 0.75$ . If the assumption of the (2 × 2) periodicity is removed, a mixed adsorption state of Ga and H should appear especially near the phase boundary obtained by using the (2 × 2) lateral cells. Hence, for a high-resolution surface phase diagram describing the surface composition more accurately, we consider that the growth surface is a mixture of Ga-atom-adsorbed and H-adsorbed areas with those coverages. For the modeling of relatively wide areas, we use (6 × 6) lateral cells (dimensions of 2 × 2 nm<sup>2</sup>). However, the Ga- or H-adsorbed atomic configurations in a (6 × 6) cell with those coverages exceed millions in number (see below), so exploration using conventional DFT calculations is unfeasible. In this Letter, we tackle this formidable task by introducing Bayesian optimization in sequential DFT calculations.

Minimization of a target quantity (energy in the present case) in multidimensional space (atomic coordinates here) is a long-standing issue. Iterative minimization,<sup>19</sup> such as the conjugate gradient occasionally combined with simulated annealing technique,<sup>20</sup> has been a typical methodology. Evolutionary algorithms are also used for several applications, including crystal-structure search.<sup>21–23</sup> However, those approaches require a huge number of iterations, thus being inappropriate for the present task. Recently, an optimization technique based on Bayesian statistics (Bayesian optimization),<sup>24</sup> which is possibly capable of predicting the minimum solution from insufficient data, has attracted attention. This technique has indeed been applied to material exploration,<sup>25–27</sup> and its validity is partly evidenced. Here, we use Bayesian optimization combined with (6 × 6) lateral-cell DFT calculations in the sequential search of nanometer-scale structures of the GaN growth surface. We reach stable structures inaccessible ever through  $\sim 10^2$  optimization trials among  $\sim 10^5$  candidates.

In this research, we explored the atomic configurations of Ga and H adatoms on a GaN(0001)–(6 × 6) surface unit cell. The surface composition corresponding to Ga<sub>ad</sub>/3Ga–H = 1/2 is considered as an example of intermediate compositions for creating a high-resolution surface phase diagram. Pure Ga<sub>ad</sub> ( $\theta_{\text{Ga}} = 0.25$ ) and 3Ga–H ( $\theta_{\text{H}} = 0.75$ ) structures have nine Ga adatoms and 27 H adatoms per (6 × 6) area, respectively. Thus, a structure to be explored has 18 H adatoms and three Ga adatoms because of the mixing ratio (Ga<sub>ad</sub>/3Ga–H) of 1/2. Choosing these pure Ga-adsorbed and H-adsorbed systems as reference systems, the stability of the structure to be explored can be expressed as the mixing enthalpy:

$$E_{\text{mix}} = E[18\text{H}3\text{Ga}] - \frac{2}{3}E[27\text{H}] - \frac{1}{3}E[9\text{Ga}], \quad (1)$$

where  $E[18\text{H}3\text{Ga}]$  is the total energy from DFT calculations of the GaN(0001)–(6 × 6) surface slab model with a surface structure to be explored and  $E[27\text{H}]$  and  $E[9\text{Ga}]$  are those of (6 × 6) surface slab models with pure 3Ga–H and Ga<sub>ad</sub> surface structures, respectively. The final target of this study is to discover a nontrivial (6 × 6) structure with a lower mixing enthalpy than simple (6 × 6) structures obtained by the patchwork of the two distinct (2 × 2) structures.

The total energies of the surface slab models were calculated based on real-space density functional theory using the RSDFT package.<sup>28,29</sup> This implementation is suitable for highly parallel computing because fast Fourier transform is unnecessary. Thus, it has an advantage, especially when applied to large-scale systems. The exchange and correlation energies were treated by the Perdew–Burke–Ernzerhof exchange correlation functional.<sup>30</sup> The nuclei and core electrons are simulated by

norm-conserving pseudopotentials.<sup>31</sup> Ga 3d electrons were treated as core electrons. The mesh spacing was taken as 0.15 Å, which corresponds to the cutoff energy of 128 Ry in the conventional plane wave basis. This set of parameters reproduce the experimental lattice constants  $a$  and  $c$  with the error of 0.2–0.4% in wurtzite GaN. A GaN(0001)–(6 × 6) surface slab model comprises a vacuum layer of more than 20 Å and GaN film (three bilayers for Bayesian exploration and five bilayers for confirmatory recalculation) with adatoms in which the bottom surface N dangling bonds are terminated by pseudohydrogens with a charge of 0.75e to mimic a semi-infinite GaN substrate.<sup>32</sup> In surface relaxation, a bottom GaN bilayer with pseudohydrogens was fixed, and the convergence criterion for the forces of  $5 \times 10^{-4}$  Hartree/a.u. (atomic unit) was used. Visualization of electron density was prepared using the VESTA package.<sup>33,34</sup>

We start with baseline models in which the (6 × 6) structures are constructed as patchworks of the two distinct structural motifs, the (2 × 2) 3Ga–H and Ga<sub>ad</sub> structures. Candidate patchwork structures are already dozens in number (combinations of three objects from a set with nine objects,  ${}_9C_3 = 84$ ). Among them, we have chosen from *our intuition* the following four structures, which represent the candidates in terms of the distribution of Ga adatoms. The (6 × 6) structures chosen are shown in Fig. 1, and the calculated mixing enthalpies are shown in Table I. In structures (a) and (b), the three Ga adatoms (red circles) are located at the vertices of small and large equilateral triangles, respectively. Structure (b), in which Ga adatoms are uniformly distributed in the whole lateral plane, is almost energetically comparable to structure (a), in which Ga adatoms are more condensed. Ga adatoms in structures (c) and (d) are on straight lines. [Note that structures (b) and (c) are identical to each other in the periodic boundary condition.] Structure (d), in which Ga adatoms are more condensed than structures (c), is the most stable, inferring that the gathering of Ga adatoms is energetically favorable.

We are now in a position to explore the stable (6 × 6) structures more completely by abandoning the (2 × 2) structural motifs. Considering the importance of the gathering of Ga adatoms obtained above, we consider a class of surface structures shown in Fig. 2, where Ga adatoms are condensed in the principal crystallographic direction. Keeping the energetically favorable coverages of H atoms and Ga adatoms, i.e.,  $\theta_{\text{Ga}} = 0.25$  and  $\theta_{\text{H}} = 0.75$ , there are 27 candidate adsorption sites for H, shown as blue circles in Fig. 2, among which 18 sites are actually covered. We do not consider symmetry constraints in this study since symmetric structures, occasionally assumed from intuition, are not necessarily most stable. Consequently, we encounter with a huge number of candidate structures, i.e.,  ${}_{27}C_{18} = 4\,686\,825$  structures.

**TABLE I.** Calculated mixing enthalpies of (6 × 6) GaN growth surfaces. (a), (b), (c), and (d): the enthalpies of the patchwork models being constructed of 3Ga–H (2 × 2) and Ga<sub>ad</sub> (2 × 2) motifs. (#130) The most stable structure discovered by the present Bayesian optimization. Values in parentheses show recalculated values using the slab models of five GaN bilayers.

Structure name	Preparation	Mixing enthalpy (eV)
a	Arrangement	0.89 (0.83)
b, c	Arrangement	0.83 (0.84)
d	Arrangement	0.54 (0.54)
#130	Bayesian Opt.	0.16 (0.13)

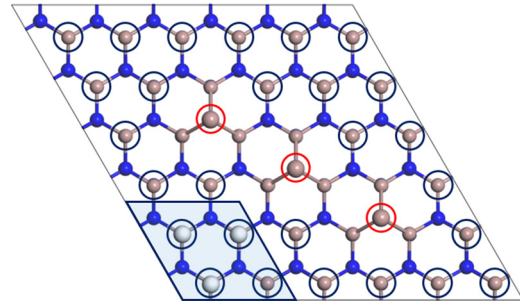


**FIG. 2.** Top view of a class of (6 × 6) surface structures to be explored by Bayesian optimization. Red circles indicate Ga adsorption sites, and blue circles indicate the candidates for 18 H adsorption sites.

This challenging exploration is performed by sequential machine learning and adaptive experimental design in the framework of Bayesian optimization. The machine learning model takes the surface structure as an input and associates it with its total energy as an output. The optimization is performed with this machine learning model that is updated by Bayesian inference. The Bayesian model allows us to obtain the predicted energy value as well as its uncertainty. Hence, the optimization generally balances sampling in domains that have not yet been explored and promising domains that have already been explored and are likely to yield good evaluation values, leading to an adaptive sampling strategy to minimize the number of function evaluations. In this study, we used an open-source Bayesian optimization library, COMBO,<sup>35</sup> in which the selection of the structure for the next trial is implemented by Thompson sampling.<sup>36</sup> In exploring the stable structures, we introduce a (2 × 2) 3Ga–H structural motif (a blue tile in Fig. 2) in the (6 × 6) structure. This does not cause loss of generality since this (2 × 2) motif is expected to be ubiquitous in real surfaces. On the other hand, this procedure reduces the number,  ${}_{27}C_{18}$ , of candidate structures to  ${}_{23}C_{15} = 490\,314$ . Each of these candidate surface structures is represented by a 23-dimensional vector in which each row corresponding to each adsorption site is filled with 1 when H is adsorbed and with 0 otherwise. This vector is the input to the machine learning model. In the COMBO implementation, the input vectors are transformed into feature vectors by a random feature map<sup>37</sup> and input to a Bayesian linear regression model,

$$E_{\text{mix}} = \mathbf{w} \cdot \phi(\mathbf{x}) + \varepsilon, \quad (2)$$

where  $\mathbf{x} \in \mathbb{R}^{23}$  is an input,  $\phi: \mathbb{R}^{23} \rightarrow \mathbb{R}^l$  is a feature map,  $\mathbf{w} \in \mathbb{R}^l$  is a weight vector, and  $\varepsilon$  is the Gaussian noise. The dimension  $l$  of the feature vector  $\phi(\mathbf{x})$  was set to 5000. This mapping is defined so that, in the limit of  $l \rightarrow \infty$ , the Bayesian linear regression model converges to a Gaussian process.<sup>35</sup> The hyperparameters were updated for each trial based on maximization of the type-II likelihood.<sup>38</sup>

Figure 3 shows the results of Bayesian optimization of the H adsorption sites, which lower the mixing enthalpy. In the early stage of the exploration, when the amount of the training data is insufficient, the mixing enthalpy is so high that it exceeds 2.5 eV. Around trial number #25, the mixing enthalpy decreases drastically, but a structure more stable than the baseline model (d) is not found yet. After that, the trend slowly decreases, indicating that sequential learning of data indeed progresses, although there are sometimes large oscillations.



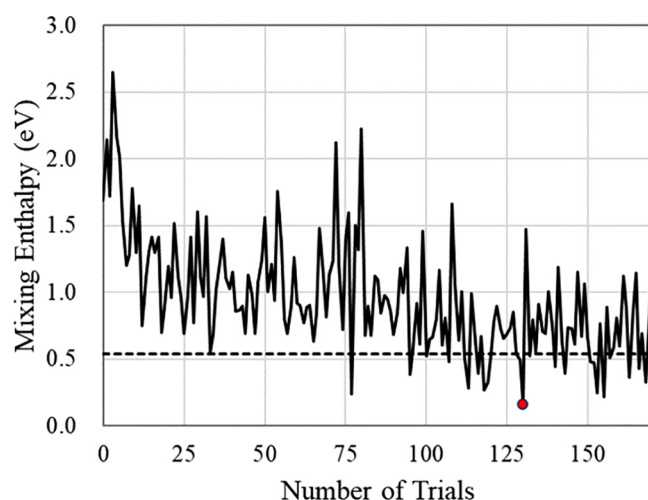


**FIG. 3.** History of the exploration of the surface structure by Bayesian optimization. The objective is to minimize the mixing enthalpy. The black dashed line corresponds to the minimum value of the baseline models, and the red marker corresponds to the most stable structure #130 in the present exploration.

After the trial number around #125, the trend appears to become saturated, so the exploration was terminated at trial number #170. In this exploration, 23 surface structures that are more stable than the baseline model have been discovered: Validity of Bayesian optimization in the present task is evidenced.

The most stable structure discovered in this exploration is structure #130. The top view of the structure is shown in Fig. 4, and its mixing enthalpy value is shown in Table I. The structure shows that H adatoms are distributed to avoid the vicinity of Ga adatoms and that the way H adatoms are distributed is asymmetric, resulting in a very complicated adsorption structure. One may tend to enumerate symmetrical structures as candidates and explore the most stable structures with limited degrees of freedom. This may be related to an ansatz that higher symmetry is favored in nature. However, such ansatz is not guaranteed in some phenomena, such as crystal growth. Hence, the

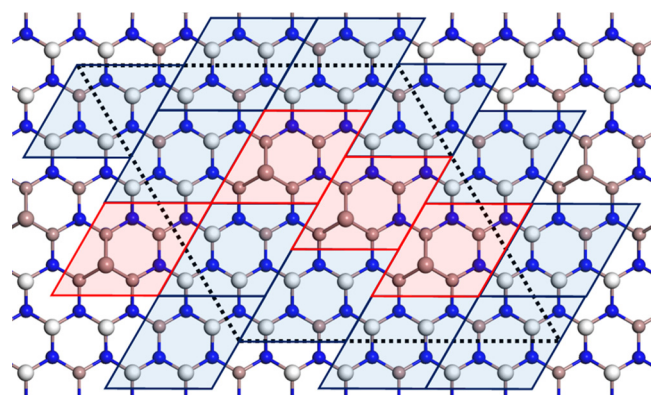


**FIG. 4.** Top view of the stable ( $6 \times 6$ ) surface structure discovered by the present Bayesian optimization (structure name #130). The black dashed tile indicates a ( $6 \times 6$ ) area.

ability to discover complicated surface structure, which lacks any symmetry, demonstrated in Fig. 4, is one of the biggest advantages of using machine learning approaches.

Next, with ECR in mind, let us carefully examine structure #130. According to ECR, when one Ga adatom or three H adatoms are adsorbed per ( $2 \times 2$ ) area in GaN(0001), one of the four topmost Ga atoms has an unoccupied dangling bond, and three of them each form a single bond with the adatom (see Fig. 5), resulting in stabilization without excess or deficiency of electrons in the bond network. In our Bayesian optimization, the structure search is not restricted to patchwork of those ( $2 \times 2$ ) structural motifs. However, the resulting structure #130 clearly shows a dense arrangement of the motifs [red tiles ( $\text{Ga}_{\text{ad}}$ ) and blue tiles ( $3\text{Ga-H}$ ) in Fig. 4] with  $3\text{Ga-H}$  motifs surrounding  $\text{Ga}_{\text{ad}}$  motifs. This finding indicates that ECR is satisfied locally in structure #130 and that further long-range electron transfer is unlikely to occur. Figure 4 shows another interesting feature: the internal configurations, i.e., the positions of the three H atoms, in  $3\text{Ga-H}$  motifs are different to each other. This suggests that the internal configuration is adjusted to reduce the interaction energy among the ( $2 \times 2$ ) motifs while ECR is still satisfied. We argue that the fully local satisfaction of ECR and the energy reduction due to the internal rearrangement in motifs, which we have found through the Bayesian optimization, are two essential ingredients to stabilize nanometer-scale GaN surfaces. These findings and the exploratory scheme will also be useful in the study of the features of other observed structures. For example, in a molecular beam epitaxy (MBE) system, where observations are possible with reflection high energy electron diffraction (RHEED) and other techniques, several longer-range ordered structures have been reported.<sup>39</sup>

In summary, we have identified the stable structure of nanometer-scale GaN (0001) surfaces with Ga- and H-adsorbates, which are the fundamental basis for crystal growth modeling, by large-scale density-functional calculations combined with machine learning Bayesian optimization technique. We have been able to reach a single stable structure with satisfactorily low mixing enthalpy by 130 trials based on Bayesian optimization among  ${}_{23}\text{C}_{15} = 490\,314$  candidate structures. We have found that the obtained structure lacks any postulated high symmetry previously introduced by human intuition, satisfies electron counting rule locally, and shows a complex adsorbate-rearrangement, leading to lower mixing enthalpy. The present scheme of Bayesian optimization combined with first-principle calculations paves a way toward identifying surface structures with a

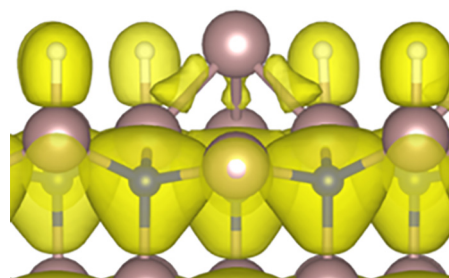


**FIG. 5.** Calculated electron density near Ga and H adatoms in the discovered structure #130. Brown, dark blue, and white atoms correspond to Ga, N, and H, respectively.

larger scale and more complex adsorbate-arrangements and then determination of surface phase diagrams for design of further preferred growth conditions.

This work was partially supported by JSPS KAKENHI (Grant No. JP20K15181) and by MEXT as “Program for Promoting Researches on the Supercomputer Fugaku” (Quantum-Theory-Based Multiscale Simulations toward Development of Next-Generation Energy-Saving Semiconductor Devices, No. JPMXP1020200205). Computational resources of the supercomputer system ITO provided by Research Institute for Information Technology, Kyushu University (Project ID hp200122) are used.

## AUTHOR DECLARATIONS

### Conflict of Interest

The authors have no conflicts to disclose.

### DATA AVAILABILITY

The data that support the findings of this study are available from the corresponding author upon reasonable request.

## REFERENCES

- H. Amano, N. Sawaki, I. Akasaki, and Y. Toyoda, “Metalorganic vapor phase epitaxial growth of a high quality GaN film using an AlN buffer layer,” *Appl. Phys. Lett.* **48**, 353–355 (1986).
- S. Nakamura, T. Mukai, and M. Senoh, “Candela-class high-brightness InGaN/AlGaIn double-heterostructure blue-light-emitting diodes,” *Appl. Phys. Lett.* **64**, 1687–1689 (1994).
- H. Otake, K. Chikamatsu, A. Yamaguchi, T. Fujishima, and H. Ohta, “Vertical GaN-based trench gate metal oxide semiconductor field-effect transistors on GaN bulk substrates,” *Appl. Phys. Express* **1**, 011105 (2008).
- T. Oka, T. Ina, Y. Ueno, and J. Nishii, “1.8 mW/cm<sup>2</sup> vertical GaN-based trench metal-oxide-semiconductor field-effect transistors on a free-standing GaN substrate for 1.2-kV-class operation,” *Appl. Phys. Express* **8**, 054101 (2015).
- T. Palacios, A. Chakraborty, S. Rajan, C. Poblenz, S. Keller, S. DenBaars, J. Speck, and U. Mishra, “High-power AlGaIn/GaN HEMTs for Ka-band applications,” *IEEE Electron Device Lett.* **26**, 781–783 (2005).
- T. Kachi, “Recent progress of GaN power devices for automotive applications,” *Jpn. J. Appl. Phys., Part 1* **53**, 100210 (2014).
- H. Amano, Y. Baines, E. Beam, M. Borga, T. Bouchet, P. R. Chalker, M. Charles, K. J. Chen, N. Chowdhury, R. Chu *et al.*, “The 2018 GaN power electronics roadmap,” *J. Phys. D* **51**, 163001 (2018).
- K. Rapcewicz, M. B. Nardelli, and J. Bernholc, “Theory of surface morphology of wurtzite GaN (0001) surfaces,” *Phys. Rev. B* **56**, R12725 (1997).
- J. Fritsch, O. F. Sankey, K. E. Schmidt, and J. B. Page, “*Ab initio* calculation of the stoichiometry and structure of the (0001) surfaces of GaN and AlN,” *Phys. Rev. B* **57**, 15360 (1998).
- T. K. Zywiets, J. Neugebauer, and M. Scheffler, “The adsorption of oxygen at GaN surfaces,” *Appl. Phys. Lett.* **74**, 1695–1697 (1999).
- C. Pignedoli, R. D. Felice, and C. M. Bertoni, “Dissociative chemisorption of NH<sub>3</sub> molecules on GaN (0001) surfaces,” *Phys. Rev. B* **64**, 113301 (2001).
- C. G. Van de Walle and J. Neugebauer, “First-principles surface phase diagram for hydrogen on GaN surfaces,” *Phys. Rev. Lett.* **88**, 066103 (2002).
- Y. Kangawa, T. Ito, A. Taguchi, K. Shiraishi, and T. Ohachi, “A new theoretical approach to adsorption-desorption behavior of Ga on GaAs surfaces,” *Surf. Sci.* **493**, 178–181 (2001).
- T. Akiyama, K. Nakamura, and T. Ito, “*Ab initio*-based study for adatom kinetics on AlN (0001) surfaces during metal-organic vapor-phase epitaxy growth,” *Appl. Phys. Lett.* **100**, 251601 (2012).
- Y. Kangawa, T. Akiyama, T. Ito, K. Shiraishi, and T. Nakayama, “Surface stability and growth kinetics of compound semiconductors: An *ab initio*-based approach,” *Materials* **6**, 3309–3360 (2013).
- P. Kempisty and Y. Kangawa, “Evolution of the free energy of the GaN (0001) surface based on first-principles phonon calculations,” *Phys. Rev. B* **100**, 085304 (2019).
- A. Kusaba, Y. Kangawa, P. Kempisty, H. Valencia, K. Shiraishi, Y. Kumagai, K. Kakimoto, and A. Koukitu, “Thermodynamic analysis of (0001) and GaN metal-organic vapor phase epitaxy,” *Jpn. J. Appl. Phys., Part 1* **56**, 070304 (2017).
- M. Pashley, “Electron counting model and its application to island structures on molecular-beam epitaxy grown GaAs (001) and ZnSe (001),” *Phys. Rev. B* **40**, 10481 (1989).
- M. C. Payne, M. P. Teter, D. C. Allan, T. Arias, and J. Joannopoulos, “Iterative minimization techniques for *ab initio* total-energy calculations: Molecular dynamics and conjugate gradients,” *Rev. Mod. Phys.* **64**, 1045 (1992).
- S. Kirkpatrick, C. D. Gelatt, and M. P. Vecchi, “Optimization by simulated annealing,” *Science* **220**, 671–680 (1983).
- D. C. Lonie and E. Zurek, “XTALOPT: An open-source evolutionary algorithm for crystal structure prediction,” *Comput. Phys. Commun.* **182**, 372–387 (2011).
- H. A. Zakaryan, A. G. Kvashnin, and A. R. Oganov, “Stable reconstruction of the (110) surface and its role in pseudocapacitance of rutile-like RuO<sub>2</sub>,” *Sci. Rep.* **7**, 10357 (2017).
- A. G. Kvashnin, D. G. Kvashnin, and A. R. Oganov, “Novel unexpected reconstructions of (100) and (111) surfaces of NaCl: Theoretical prediction,” *Sci. Rep.* **9**, 14267 (2019).
- J. Snoek, H. Larochelle, and R. P. Adams, “Practical Bayesian optimization of machine learning algorithms,” *Adv. Neural Inf. Process. Syst.* **25**, 2921–2959 (2012), available at <https://proceedings.neurips.cc/paper/2012/file/05311655a15b75fab86956663e1819cd-Paper.pdf>.
- A. Seko, A. Togo, H. Hayashi, K. Tsuda, L. Chaput, and I. Tanaka, “Prediction of low-thermal-conductivity compounds with first-principles anharmonic lattice-dynamics calculations and Bayesian optimization,” *Phys. Rev. Lett.* **115**, 205901 (2015).
- S. Ju, T. Shiga, L. Feng, Z. Hou, K. Tsuda, and J. Shiomi, “Designing nanostructures for phonon transport via Bayesian optimization,” *Phys. Rev. X* **7**, 021024 (2017).
- Z. Hou, Y. Takagiwa, Y. Shinohara, Y. Xu, and K. Tsuda, “Machine-learning-assisted development and theoretical consideration for the Al<sub>2</sub>Fe<sub>3</sub>Si<sub>3</sub> thermoelectric material,” *ACS Appl. Mater. Interfaces* **11**, 11545–11554 (2019).
- J.-I. Iwata, D. Takahashi, A. Oshiyama, T. Boku, K. Shiraishi, S. Okada, and K. Yabana, “A massively-parallel electronic-structure calculations based on real-space density functional theory,” *J. Comput. Phys.* **229**, 2339–2363 (2010).
- Y. Hasegawa, J.-I. Iwata, M. Tsuji, D. Takahashi, A. Oshiyama, K. Minami, T. Boku, H. Inoue, Y. Kitazawa, I. Miyoshi *et al.*, “Performance evaluation of ultra-large-scale first-principles electronic structure calculation code on the K computer,” *Int. J. High Perform. Comput. Appl.* **28**, 335–355 (2014).
- J. P. Perdew, K. Burke, and M. Ernzerhof, “Generalized gradient approximation made simple,” *Phys. Rev. Lett.* **77**, 3865 (1996).
- N. Troullier and J. L. Martins, “Efficient pseudopotentials for plane-wave calculations,” *Phys. Rev. B* **43**, 1993 (1991).
- K. Shiraishi, “A new slab model approach for electronic structure calculation of polar semiconductor surface,” *J. Phys. Soc. Jpn.* **59**, 3455–3458 (1990).
- K. Momma and F. Izumi, “VESTA: A three-dimensional visualization system for electronic and structural analysis,” *J. Appl. Crystallogr.* **41**, 653–658 (2008).
- K. Momma and F. Izumi, “VESTA 3 for three-dimensional visualization of crystal, volumetric and morphology data,” *J. Appl. Crystallogr.* **44**, 1272–1276 (2011).
- T. Ueno, T. D. Rhone, Z. Hou, T. Mizoguchi, and K. Tsuda, “COMBO: An efficient Bayesian optimization library for materials science,” *Mater. Discov.* **4**, 18–21 (2016).
- O. Chapelle and L. Li, “An empirical evaluation of thompson sampling,” *Adv. Neural Inf. Process. Syst.* **24**, 2249–2257 (2011), available at <https://proceedings.neurips.cc/paper/2011/file/e53a0a2978c28872a4505bdb51db06dc-Paper.pdf>.
- A. Rahimi and B. Recht, “Random features for large-scale kernel machines,” *Adv. Neural Inf. Process. Syst.* **3**, 1177–1184 (2007).
- C. E. Rasmussen, “Gaussian processes in machine learning,” in *Summer School on Machine Learning* (Springer, 2003), pp. 63–71.
- A. Smith, R. Feenstra, D. Greve, M.-S. Shin, M. Skowronski, J. Neugebauer, and J. Northrup, “Determination of wurtzite GaN lattice polarity based on surface reconstruction,” *Appl. Phys. Lett.* **72**, 2114–2116 (1998).